Research article

Adrenergic to mesenchymal fate switching of neuroblastoma occurs spontaneously in vivo resulting in differential tumorigenic potential

Maria C. Lecca[1], Marianne A. Jonker[2], U. Kulsoom Abdul[4], Asli Küçükosmanoglu[4], Wessel van Wieringen[2,3], Bart A. Westerman[1,4,*]

[1] Department of Oncogenomics, Amsterdam Medical Center (AMC), the Netherlands
[2] Department of Epidemiology and Biostatistics, VU University Medical Center, Amsterdam
[3] Department of Mathematics, VU University, Amsterdam, De Boelelaan 1081a, 1081 HV Amsterdam
[4] Department of Neurosurgery, Cancer Center Amsterdam, VU University Medical Center, Amsterdam

*Correspondence: a.westerman@vumc.nl (Bart A. Westerman)

https://doi.org/10.31083/j.jmcm.2018.04.4221

Abstract

Neuroblastoma is a pediatric tumor that originates from cells of the adrenergic lineage. Here we investigated the balance between differentiation and dedifferentiation in relation to tumor-engraftment potential in preclinical mouse models. We analyzed intratumoral heterogeneity through comparison of marker expression of normal adrenergic development versus tumor marker expression, which showed the presence of sympathoadrenal as well as mesenchymal subtypes of neuroblastomas cells. Subsequently, we evaluated long-term outgrowth capacity of these two (FACS-sorted) cell populations, which showed that adrenergic cells have a stronger long-term clonogenic potential. Engraftment of these sorted populations into mice revealed the occurrence of heterogeneous populations. Modelling of the interconversion rate indicated that cell fate transitions from the adrenergic to mesenchymal state were obtained gradually and stochastically as the tumors grew in mice. We found that adrenergic cells have an increased tumorigenic potential in mice without signs of beneficial cross talk between the two lineage populations. These findings indicate that neuroblastoma contains two rivalling differentiation states that exhibit differences in long term clonal/tumorigenic potential. We expect these states to be relevant for therapy resistance as a result of intratumoral heterogeneity.

Submitted: November 22, 2018; **Revised:** December 9, 2018; **Accepted:** December 15, 2018

1. Introduction

Neuroblastoma is a devastating childhood disease that effects the adrenal glands and peripheral nerves [1]. The disease leads to relapses in 40% of the patients through therapy resistance [2] for which intratumoral heterogeneity is considered to be accountable.

The development of neuroblastoma is comparable with the normal neuroendocrine system development. Neuroblastoma occurs at 90% of cases in the adrenal gland and retroperitoneal paraspinal ganglia, the region of the developing adrenal medulla and surrounding tissues. It is also found along the sympathetic ganglia [3, 4]. It has been shown that high MYCN expression driven by sympathoadrenal lineage-determining genes, such as DBH and TH, can give rise to neuroblastomas. Therefore, it is believed that neuroblastoma might arise in differentiated as well as less differentiated cells of the adrenergic lineage.

Morphological and behavioural heterogeneity has been recognized in a growing number of malignant tumors including neuroblastoma [5]. This heterogeneity is often associated with therapy resistance [6]. Histologically, neuroblastic tumors display different degrees of ganglioneuronal differentiation ranging from highly malignant neuroblastic tumors with no signs of ganglioneuronal differentiation to a benign tumor. The fully matured end of the spectrum consists of fully differentiated ganglioneuroma. In addition, neuroblastoma is known to be a heterogeneous tumor, based on morphological differences. More recently, we showed that adrenergic-to-mesenchymal transition occurs in neuroblastoma, which could have important implications for therapy [6].

To gain a better understanding of neuroblastoma intratumoral heterogeneity and cell fate interconversion, we herein provide a systematic analysis. We show that cell identity interconversion occurs stochastically during tumor expansion and consists of two relatively stable states. Furthermore, we show that the clonal expansion and tumorigenic potential of adrenergic neuroendocrine cells are much stronger than mesenchymal cells. These experiments provide an insight into the balance of cell identity versus tumor engraftment in neuroblastoma.

2. Results

2.1. *tNSE clustering of pediatric tumor cell lines distinguishes between a neuronal and mesenchymal lineage in neuroblastoma*

As above mentioned, the heterogeneity of neuroblastoma is based on morphological differences between cell lines. Since pediatric tumors are often driven by aberrant activation of developmental pathways, we argued that neuroblastoma tumor heterogeneity might be reflected in the overlap with transcriptional programs present in pediatric malignancies. We therefore performed tSNE clustering of the cell lines derived from the following six pediatric tumors: medulloblastoma, neuroblastoma, pediatric acute lymphoblastic leukemia (ALL), Ewing sarcoma, osteosarcoma and rhabdomyosarcoma. This

resulted in clusters of distinct groups according to their organ of origin (Figure 1). These data were independently confirmed by performing K-means clustering (Figure S1A) and principal component analysis (PCA, Figure S1B). The majority of neuroblastoma cell lines clustered together with the neuroectodermally-derived medulloblastoma cell lines as expected. However, a number of neuroblastoma and medulloblastoma cases clustered together with cell lines of mesenchymal origin (Ewing sarcoma, osteosarcoma and rhabdomyosarcoma). These data indicate that neuroblastoma cells might have similarities to neuronal- but also to mesenchymal-like features and suggests that these cell lines may be heterogeneous.

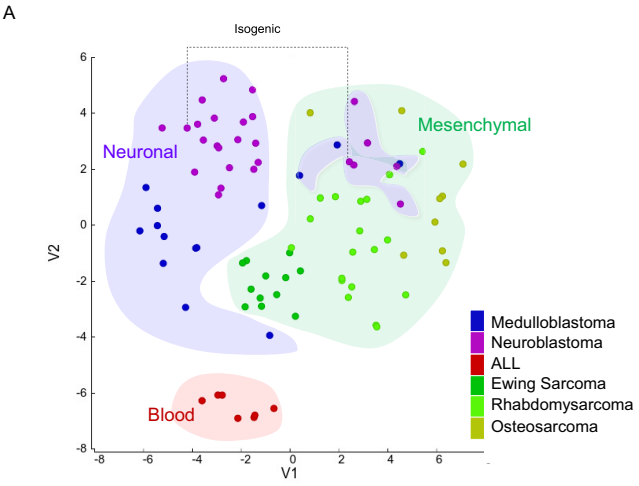

Fig. 1. A number of neuroblastoma cell lines resemble tumors of mesenchymal origin. tSNE clustering of mRNA expression data of 87 pediatric tumor cell lines consisting of the neuronal tumors medulloblastoma ($n = 14$), neuroblastoma ($n = 26$), tumors of mesenchymal origin, Ewing Sarcoma ($n = 21$), rhabdomyosarcoma ($n = 19$) and osteosarcoma ($n = 9$) and the blood derived tumor type ALL ($n = 7$). The three main clusters observed are neuronal tumors (blue), mesenchymal tumors (green) and blood ALL (red). Note that some neuroblastoma and medulloblastoma cell lines cluster together with tumors of mesenchymal origin. Perplexity of the clustering was 28. Isogenic pair: SHEP2 and SY5Y.

2.2. *Lineage marker analysis shows that neuroblastoma cell lines represent multiple stages of neural crest development*

To further investigate the relation of adrenergic/neuronal and mesenchymal cell fates within and between tumors of individual patients, we first analyzed the expression levels of markers of the most important stages of neural crest development. Next, we analyzed pan-neuronal markers and mesenchymal markers summarized in Figure 2A [7, 8]. Our data show that adrenergic neuroblastoma cells express markers of catecholamine biosynthesis such as TH and Chromogranin A (Figure 2B and Figure 4D), indicating that the cells have matured to a sympathetic neurons or a chromaffin state. Pan-neuronal markers, such as βIII tubulin as well as the proneural specifier ASCL1, were positive in the neuronal subtype of cells as expected. Furthermore, the expression of neurofilament light (NEFL) expression suggests a shift towards a sympathoadrenal fate rather than a chromaffin fate [8]. Interestingly, our subset of mesenchymal cell lines has high mRNA levels of markers reflecting migratory and post-migratory neural crest cells (Figure 2A), but lacking any markers of sympathoadrenal commitment. Immunostaining and RNA profiling of isogenic cell lines 691T, 691B, SHEP2 and SY5Y confirmed these findings (data not shown). Furthermore, the mesenchymal cell line 691T expressed neural crest stem cell markers, SOX9, p75NGFR (Figure 1E) and lacked expression of the neuroendocrine marker TH. These mesenchymal, neural crest stage-like cells also lack mRNA expression of WNT1, CDH1 and SOX10, markers of pre-migratory, neural crest cells that have not yet delaminated (data not shown). This analysis formed the basis for the definition of the mesenchymal group of neuroblastoma cells that we previously published [6]. Here we additionally show a gene expression profile that highly overlaps with migratory and post-migratory neural crest cells of human embryos at stages CS12-CS18.

2.3. *Mesenchymal and adrenergic lineage cells differ in their tumorigenic potential and can interconvert spontaneously in vivo*

Mesenchymal and adrenergic cells are found together in almost all neuroblastoma tumors [6]. They share the same genetic defects, implying a shared descent. However, it is unknown whether cell intrinsic or exogenous signals trigger a cell-fate interconversion. AMC700B and AMC711T cell lines express both mesenchymal and neuroendocrine markers. By performing mRNA expression analysis of CD133/CD24-FACS sorted cells we found that this distinction that was found between adrenergic and mesenchymal subpopulations, is also present in cell lines. We found mutually exclusive expression of cell fate markers in mesenchymal (CD133+) and adrenergic (CD133-) sorted populations, which was confirmed by qPCR analysis (Figure 3A).

To determine whether mesenchymal and adrenergic sorted populations differed in the clonal outgrowth capability, we performed single cell clonal expansions of the 700B and 711T primary cell lines after FACS sorting. The CD133- lines resembled cells committed to a sympathoadrenal fate and accordingly expressed neuroendocrine (adrenergic) markers such as PHOX2B, DBH and TH. In contrast, CD133+ lines resembled migratory neural tube precursor cells that lacked these markers, but expressed mesenchymal markers such as p75NGFR, SLUG, VIM and FN1. The two mesenchymal and adrenergic populations did not markedly differ in their cell cycle profile (Figure 3B), but showed differences in clonal outgrowth capacity (Figure 3C). Sympathoadrenal cultures had a vital appearance (Figure 3C). To quantify the clonal expansion capacity, cells were plated as single cells in 384 wells plates and serially passed to a well with a larger surface area when they reached near confluence as shown in Figure 3D. Clonal outgrowth occurred at a low frequency (Figure 3E) and clonal expansion of adrenergic (CD133-) cells was efficient and led to long-term expandable cultures (LT, Figure 3F). Effects were independent of adherent or sphere growth (data not shown). Single cell outgrowth of mesenchymal cells (CD133+) only led to cultures with a short-term expandable culture (ST, Figure 3F). Accordingly, the sphere cultures showed a necrotic appearance (Figure 3C, lower panels). By performing titrations of cell densities toward clonal outgrowth conditions (1,000 cells/cm^2), the adrenergic (CD133-) population showed more clonal expansion potential as expected (Figure 3G).

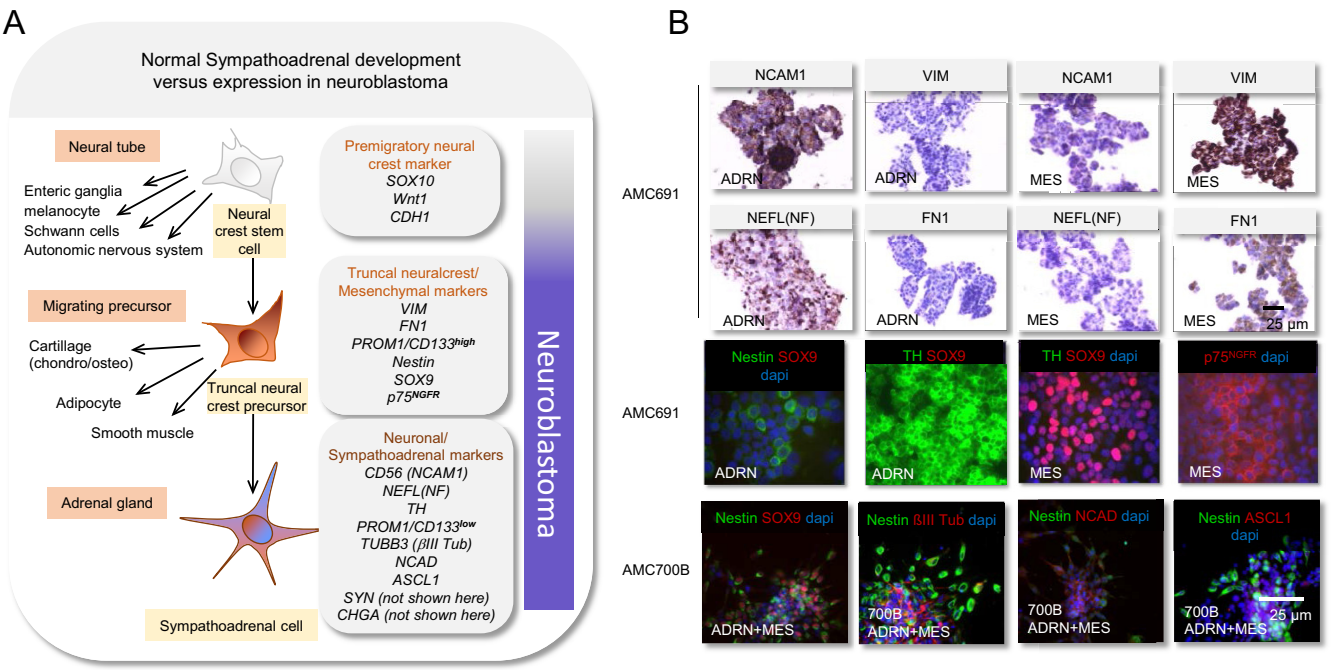

Fig. 2. Neuroblastomas express markers of normal sympathoadrenal differentiation. (A) Schematic visualization of neural crest to sympathoadrenal differentiation. Neuroblastomas show expression of mesenchymal and adrenergic stages but not of premigratory neural crest stages (B) Immunostainings of primary cultures of neuroblastoma patients. Cells were stained with antibodies that were suited for IHC of paraffin embedded cells (upper panels) or immunofluorescence of cells grown onto glass slides (lower panels).

2.4. *In vivo transplantations show spontaneous lineage conversion and differences in tumorigenesis*

Since the *in vitro* experiments showed cell autonomous differences in clonal outgrowth capacity, we tested the tumor-initiation capacity of the isogenic cell lines derived from patients AMC700 (Figure 4A), AMC691 and SKNSH. Consistently with the *in vitro* data, adrenergic type cells have stronger tumorigenic potential (Figure 4B).

We next tested whether the cell-autonomous heterogeneity of developmental states and clonogenic potential were also occurring *in vivo*. Xenotransplantation of mesenchymal/adrenergic FACS-sorted cells into nude mice gave rise to heterogeneous tumors as shown by VIM, SYN and CHGA expression resulting in patchwork-like pattern of adrenergic and mesenchymal areas in the tumors (Figure 4C, D). This indicates that a delicate balance exists between maintenance and loss of cell identity during clonal expansion.

2.5. *Modelling of lineage conversion shows that interconversions occur spontaneously and randomly*

We next investigated the kinetics of the interconversion *in vivo* by modelling the evolutionary process using a clonal evolution model (Figure 5A). Prior to this experiment, we determined the growth rate of adrenergic and mesenchymal cells, assuming this growth rate remains constant during the subsequent *in vivo* experiments. Tumors emanating from an adrenergic origin generated mesenchymal progeny and *vice versa* (Figure 5B). As we measured the size of each clonal population during the marker analysis, we could extrapolate at which time point lineage interconversion occurred. None of the clones that occurred after injection of sympathoadrenal cells had a size that indicated that they existed at the moment of tumor initiation (Figure 5C, D). In contrast, tumors derived from these mesenchymal lineage cells showed an early onset appearance of sympathoadrenal clones, consistent with their higher tumorigenicity as was observed *in vitro* (Figure 5B) as well as *in vivo* (data not shown). Given all assumptions, these findings indicate that stochastic events control the *in vivo* identity behaviour of the tumor cells.

Subcutaneous co-injection of small cell lung cancer mesenchymal and neuroendocrine cell lines in immunodeficient mice revealed a crucial role for these cells in the formation of distant metastases [9]. Nonetheless, strong evidence also suggests that metastatic biopsies are often differentiated and do not express markers that are different from their primary tumors [10–12]. We therefore determined whether co-injection of sympathoadrenal cells and mesenchymal cells influenced the tumorigenic potential. The results showed no significant difference between mice that received the co-injection in two different flanks versus co-injected cells in one flank (Figure S2). Mesenchymal cells did not have the ability to grow out *in vivo*. These data show that co-injection of mesenchymal and sympathoadrenal neuroblastoma cells *in vivo* does not affect the tumorigenic potential.

Collectively, our results show that two cell populations exist in neuroblastoma cultures where the sympathoadrenal counterpart is more tumorigenic. Nonetheless, sympathoadrenal tumors interconvert partially to mesenchymal lineage cells with a low frequency and these clonal populations occur spontaneously after tumor initiation.

3. Discussion

Based on the expression of lineage markers in neuroblastoma cell cultures and xenografted tumors, we have generated a lineage model showing the developmental stage to which neuroblastoma is restricted (Figure 2A). This model shows that cells from the mesenchy-

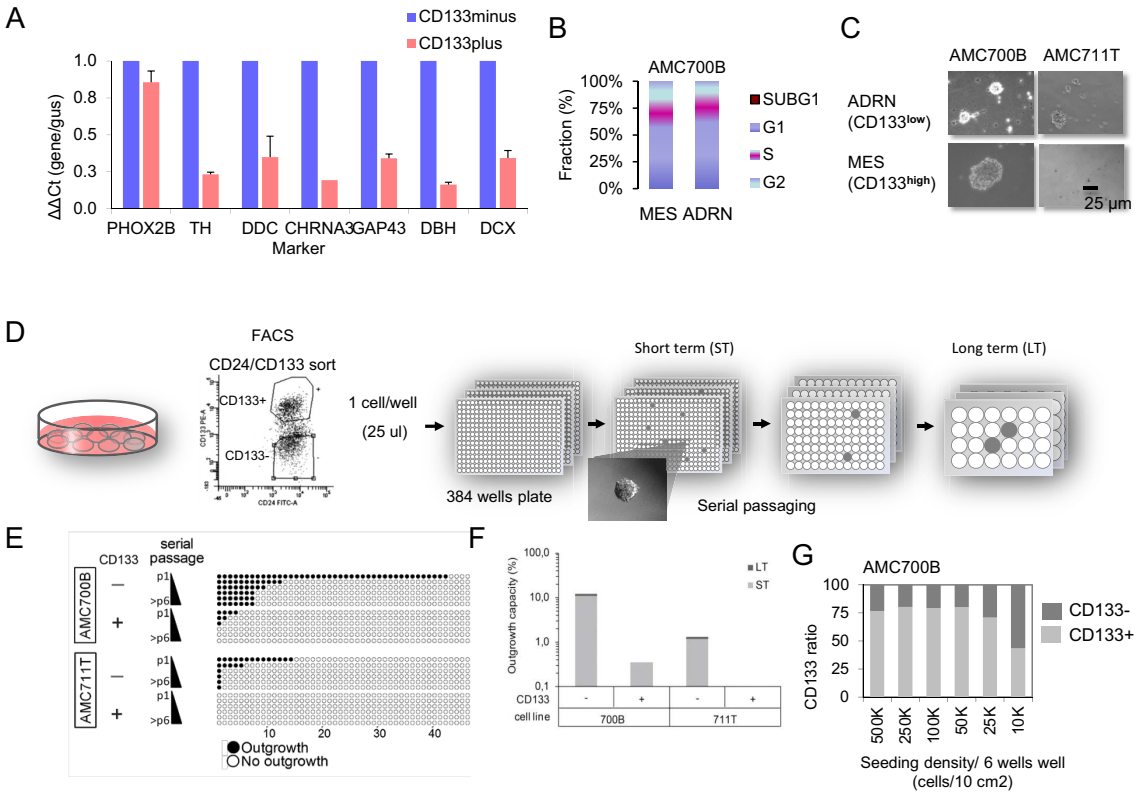

Fig. 3. Sympathoadrenal neuroblastoma cells have a long term clonal expansion capacity. (A) qPCR data showing that FACS sorted AMC700B cells for CD133 expression shows that MES (CD133 +) cells have lower expression of ADRN genes. (B) Cell cycle profile based on click it FACS analysis showing that MES and sympathoadrenal cells have a similar cell cycle profile. (C) Light microscopy of FACS sorted mesenchymal and sympathoadrenal cells showing that sympathoadrenal cells have a viable morphology in contrast to the mesenchymal cells. (D) Schematic outline of the clonal expansion experiment. Cells were FACS sorted for CD133/CD24 staining and plated for clonal outgrowth into 384 wells plates. Each well was checked for the presence of maximal one sorted cell. Cells were serially expanded and assayed for CD133 expression. (E) Clonal outgrowth and serial expansion of CD133-700B cells (NE type) occurred more frequent than clonal outgrowth of CD133+ cells (MES type). NE cells could be serially expanded for multiple passages leading to long term cultures. (F) Histogram showing the relative amount of short term expanding cultures versus long term expanding cultures. CD133-NE type neuroblastoma cells show long term expanding cultures only. (ST) Short term clonal capacity (in percentage), (LT) long term clonal capacity are the chances to generate a culture from a single cell that lasts for less or more than 5 passages, respectively. (G) Titration of the number of cells per 6 wells results in enrichment of CD133-cells upon lower seeding densities that required clonal outgrowth after two week of expansion.

mal stage (p75NGFR and SOX9 delaminated neural crest marker positive, Wnt1 and NCAM neural crest marker negative; data not shown) can differentiate towards the sympathoadrenal neuroendocrine lineage (ASCL1, PHOX2B and HAND1 neuroendocrine marker positive) and *vice versa.* Cancer cells with a mesenchymal-like undifferentiated phenotype are known to be potentially involved in the development of invasive and drug resistant aggressive tumors [10, 13–15].

Early studies evaluating neuroblastoma cell heterogeneity have documented the presence of neuroblastoma cell lines lacking the neuroendocrine features which are commonly observed in tumors [16] (Ciccarone et al., 1989, Ross et al., 1995). These authors hypothesized the existence of a common ancestor cell representing a malignant neural crest stem cell (I-type) able to self-renew and give either a neural (N) or a non-neural (S) daughter cell. Our results indicate that the developmental lineage heterogeneity observed in neuroblastoma is not the result of a hierarchical organization of cancer stem cells (i.e. the I, N, S model) but rather as a result of stochastic oscillation between two lineage states.

In our mice experiments, the initial lineage identity remained dominant during the *in vivo* evolution for both adrenergic and mesenchymal type cells. This tendency to maintain the initial state might be driven by self-reinforcing mechanisms and is apparently dominant over the stochastic evolutionary cell identity process. Our findings show that mesenchymal neuroblastoma cells have a poorer *in vivo* and *in vitro* tumorigenicity which is in line with earlier observations that showed that mesenchymal neuroblastomas are less tumorigenic [5, 17–21].

Taken together, our results show that neuroblastoma cell lines are heterogeneous and contain subpopulations of cells reminiscent of the delaminated mesenchymal cells that migrate from the neural tube and cells that have adopted a sympathoadrenal fate that are reminiscent of cells that have arrived at the dorsal root ganglion in order to differentiate.

4. Materials and Methods

4.1. *In silico analysis*

tSNE (T-distributed Stochastic Neighbour Embedding) clustering was performed on mRNA expression data of MAS5.0 normalized U133p2 data using R2 using the standard settings. Non-

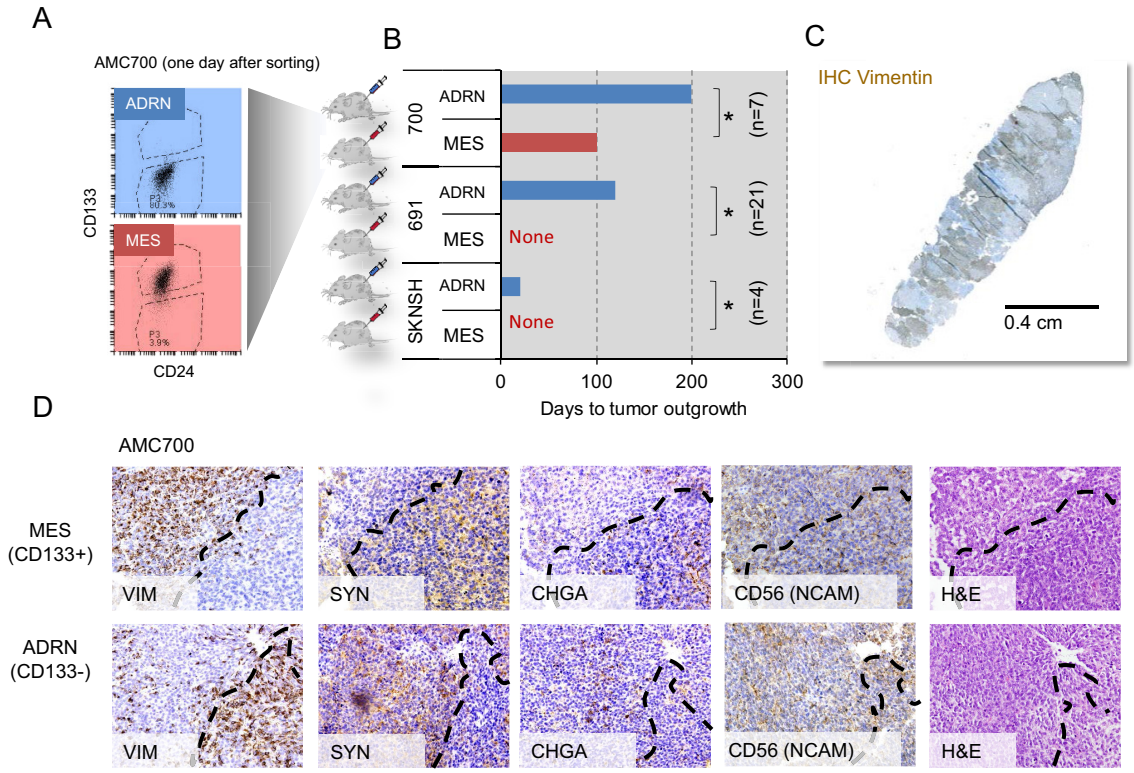

Fig. 4. Sympathoadrenal neuroblastoma cell cultures are more tumorigenic. (A) FACS plot of CD133/CD24 contained cells one day after sorting B) Average survival of mice when ADRN and MES type cells are compared from three isogenic pairs (200,000 cells [AMC700B]; 5x10^6 [AMC691] and 1x10^6 [SKNSH] were injected). (C) Macroscopic image of immunohistochemistry for vimentin showing a patchwork pattern of vimentin positive and negative domains. (D) Immunostainings of primary cultures of neuroblastoma patients. Cells were stained with antibodies that were suited for IHC of paraffin embedded cells (upper panels) of immunofluorescence of cells grown onto glass slides (lower panels). *$p < 0.05$ log rank test.

hierarchical K-means clustering analysis was done on MAS5.0 normalized U133p2 microarray datasets using an appropriate amount of groups. For the clustering analysis of the panel of the ITCC consortium cell lines, the top 100 genes were taken for clustering into four groups. For K-means clustering the 39 cell lines that include neuroblastomas and osteosarcoma, the top 60 of genes were taken. Source: R2.amc.nl/ps_itcc_cellpanel87_u133p2.

4.2. *Cell lines*

Primary cell lines have been characterized by Bate-Eya et al., 2013 [22]. Cell lines were derived either from primary tumors (indicated by T) or bone marrow metastases (indicated by B) and cultured in DMEM/F12 including 10 ng/ml bFGF (Peprotech), 20 ng/ml EGF (BD), penicillin and streptomycin (50 units of penicillin [base] and 50 μg of streptomycin [base]/ml, Thermo Fisher). Classical neuroblastoma cell lines were grown in DMEM without glutamine supplemented with non-essential amino acids, 10% FCS as well as penicillin and streptomycin (50 units of penicillin [base] and 50 μg of streptomycin [base]/ml, Thermo Fisher).

4.3. *FACS sorting*

CD133/CD24 sorting was performed using CD133/2 (293C3)-PE (miltenyibiotec #130-090-853) or APC antibodies in a 1: 10 dilution using isotype controls. CD24 is a neuronal marker that can be used to distinguish neural sub-fractions within a CD133 positive population (pelicluster CD24, Sanquin M1605, isotype control Pelicluster IgG1 FITC, Sanquin M1453). The day after sorting, single cell colony outgrowth was performed by dissociating sphere cultures. Individual cells were plated into 384 well assay and tissue culture plate Black/Clear/TC/Sterile/Lid plates (BD Biosciences #353270). Plating of individual cells were visually confirmed. Cells were expanded into colonies that were serially passaged using all grown cells whenever near confluence was reached. Colony passaging was performed from consecutively from 384 wells plate wells to 96, 48, 24, 12, 6 wells plate wells from which long term cultures were started. Passage numbers are shown in Figure 3E.

4.4. *In vivo experiments*

Nude mice (Harlan laboratories) were subcutaneously injected with FACS sorted cell lines (200,000 cells each in 200 μl [700B] or 5x10^6 cells in 100 μl [691T and B]) in a 50% matrigel (BD #354234)/PBS solution. After tumor outgrowth up to 1 cm^3, mice were sacrificed using cervical translocation under anaesthesia. Tumors were processed for paraffin embedding as well as snap frozen for immunofluorescence microscopy. All experiments were conducted under approval of the ethical board of the Academische Medische Centrum in Amsterdam.

4.5. *Detection methods*

For immunohistochemistry, cells and tissues were fixed overnight in 10% neutral buffered formalin. Antigen retrieval was performed by boiling in sodium citrate (10mM Sodium Citrate, 0.05% Tween

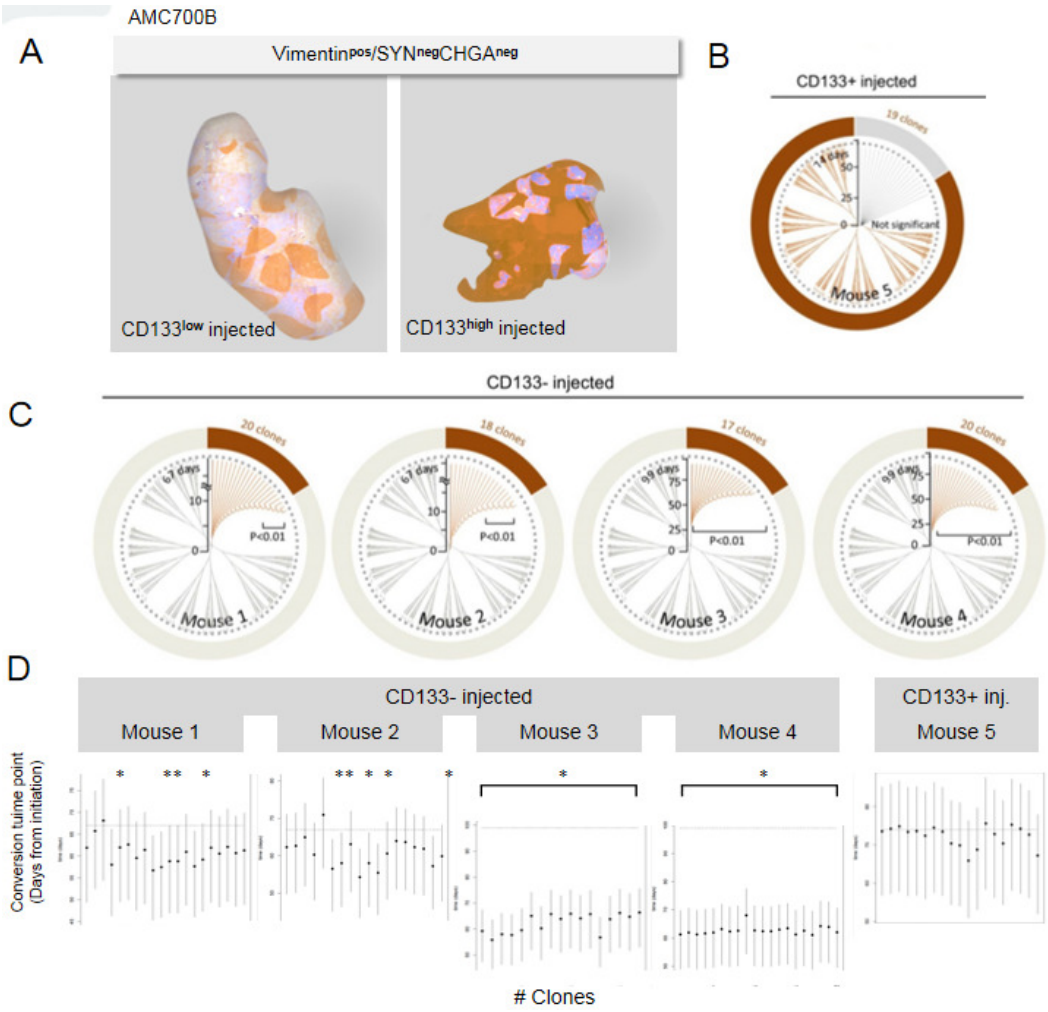

Fig. 5. Cell fate interconversion occurs stochastically in vivo. (A) Injection of CD133^{low} as well as CD133^{high} cells gave rise to heterogeneous tumors as shown by expression of the MES identifier: VIM (shown in brown) with mutual exclusive absence of expression of SYN and CHGA in these clones. (B) Circos plots representative of the clonal evolution analysis where the moment of establishment of the intratumoral heterogeneity was estimated from clone size. When MES cells were injected, occurrence of MES negative clones was overlapping with the time of tumor initiation, consistent with the tumor outgrowth phenotype that was determined based on the previous in vitro and in vivo experiments. (C) Circos plots showing that many clones that were derived from sympathoadrenal cells converted to a mesenchymal fate. (D) These clones were formed significantly later than the time point of tumor injection of the tumor, i.e. the occurrence of mesenchymal population is uncoupled from the tumor initiation. Significant cases are shown by an Asterix.

20, pH 6.0) buffer for 20 min. The following primary antibodies were used: Vimentin (VIM), Synaptophysin (SYN) and Chromogranin A (CHGA). For Western blot detection, the following antibodies were used: Vimentin, Cell Signaling #5741; Slug (C19G7), Rabbit mAb Cell Signaling 9585; Fibronectin antibody, R&D systems AF1918; DBH (Cell Signaling 8586s); PHOX2B (Santa Cruz sc-376997); TH (Santa Cruz sc-25269); MYCN (Pharmingen clone B8.4. B); alpha Tubulin (Cell Signalling sc-3873). For qPCR, total RNA isolation was performed using Trizol (Life Sciences) followed by SYBR green qPCR analysis (Bio-Rad #170-8880) using primers that were tested and compared to control RNA samples that showed differential expression of the genes analysed.

4.6. *Phenotypic clonal evolution analysis and gene signatures*

For mice injected with either CD133- cell or CD133+ 700B cells, the following information was available: (1) tumor cell type injected, (2) the number of tumor cells injected, (3) time (in days) from injection to harvest, (4) number of cells constituting the harvested tumor, (5) number of clones found in the harvested tumor, and (6) number of cells constituting each clone. In total n mice were injected with each x tumor cells. For every mouse, a tumor was detected after a certain time, only if at least one of the injected cells grew out to a tumor. Define $Y_1, \ldots, Y_n$ as n indicator functions, with Y_i equal to 1 if in mouse i a tumor has been detected and 0 otherwise. In order to compute the probability that Y_i equals 1, in mouse i a tumor is detected, we define $X_1, \ldots, X_{mi}$ as m_i indicator functions with X_j equal to 1 if, in mouse i, cell j grows out to a tumor and 0 otherwise. We assume that $X_1, \ldots, X_{mi}$ are independent in the sense that if cell j grows out to a tumor, this does not have any effect on the outgrow of the other cells. p is defined as the probability where $p := \mathrm{P}(X_j = 1)$. Then, $\mathrm{P}(Y_i = 0)$ and $\mathrm{P}(Y_1 = 1)$ can be computed in

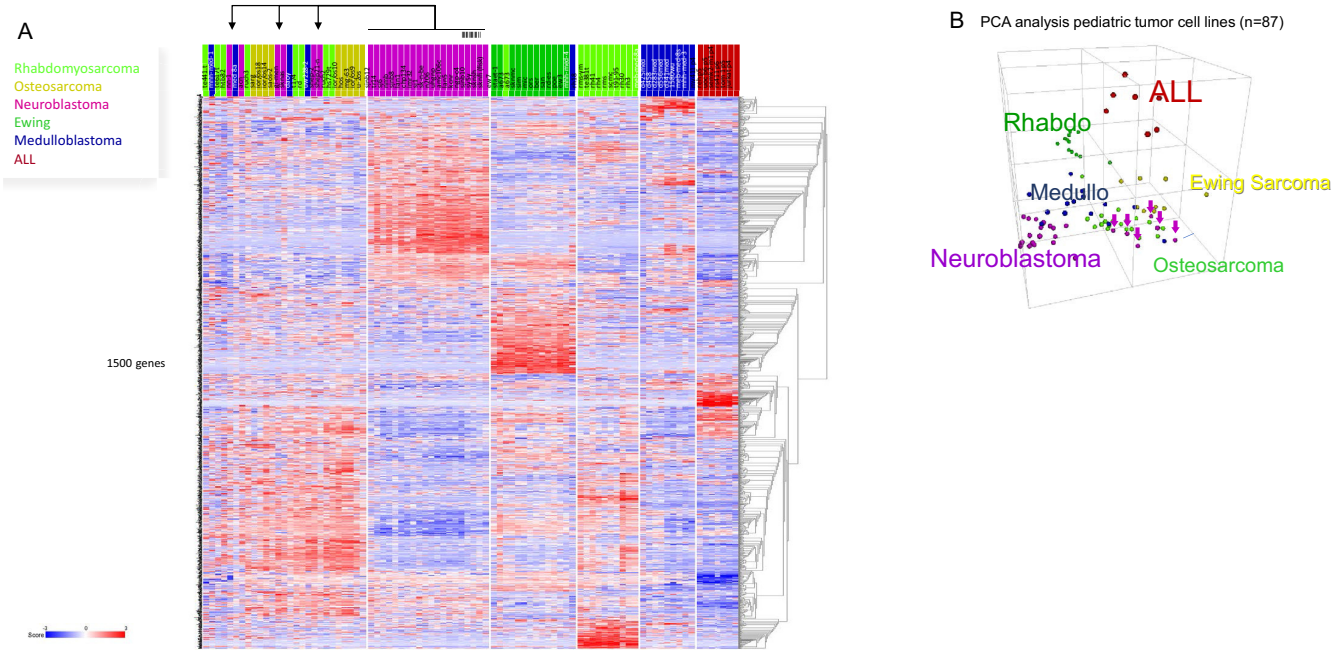

Fig. S1. K-means clustering shows that some neuroblastoma cell lines cluster together with tumors of a mesenchymal origin. (B) PCA plot showing that some neuroblastoma cell lines cluster together with tumors of a mesenchymal origin (purple arrows).

terms of p as follows:

$$\mathrm{P}(Y_i = 0) = \mathrm{P}(X_1 = 0, \ldots, X_{m_i} = 0) = \prod_{j=1}^{m_i} \mathrm{P}\left(X_j = 0\right) = (1-p)^{m_i}.$$

Consequently, the probability $\mathrm{P}(Y_i = 1) = 1 - (1-p)^{mi}$. This holds for $i = 1, \ldots, n$. Supposing we observe the data $y_1, \ldots, y_n$, then p can be estimated with the method of maximum likelihood. The likelihood is given by:

$$\prod_{i=1}^{n} [1 - (1-p)^{m_i}]^{y_i} [(1-p)^{m_i}]^{1-y_i}.$$

Maximizing this product with respect to p yields the maximum likelihood estimate of p. The uncertainty in the maximum likelihood estimate of p is assessed through re-sampling. Thousand nonparametric bootstrap samples are drawn from the original data. No distinction between the cell type with respect to p can be made due to the inserted mixture of cell types.

To estimate the cell division rate, an exponential growth model was used. Hence, for mouse i (injected with CD133+ tumor cells) the total number of cells at time t (in days) is the fraction of injected cells that proliferates times 2 to the power growth rate times the elapsed time. In formula:

$$N_{i,\mathrm{CD133+}}(t) = \left(pn_{i,\mathrm{CD133+}} 2^{\mathrm{init}}\right)^{r_{\mathrm{CD133+}} t},$$

in which $N_{i,\mathrm{CD133+}}(t)$ is the number of tumor cells at time t, p the probability of a tumor cell proliferating, $n_{i,\mathrm{CD133+}}$ the number of injected CD133+ tumor cells, $r_{\mathrm{CD133+}}$ the proliferation rate (per day). With the left-hand side observed in the experiment, the rate parameter may be estimated using a least squares approach:

$$\hat{r}_{\mathrm{CD133\text{-}}} = \arg \min_{r_{\mathrm{CD133\text{-}}>0}} \sum_{i=1}^{4} \left[\log_2\left(n_{i,\mathrm{CD33\text{-}}}\right) - \log_2\left(pn_{i,\mathrm{CD133\text{-}}}^{\mathrm{init}}\right) - r_{\mathrm{CD133\text{-}}} t_i\right]^2.$$

In the above the estimate of parameter p as obtained above is plugged in. For the assessment of the uncertainty of the rate parameter estimate, it is re-estimated by simultaneously *i*) sampling a p from its above constructed distribution and *ii)* re-sampling the mice non-parametrically with replacement. For the mouse injected with CD133-tumor cells, a similar model is assumed and the proliferation rate of these cells is estimated as:

$$\hat{r}_{\mathrm{CD133\text{-}}} = \arg \min_{r_{\mathrm{CD133\text{-}}>0}} \sum_{i=1}^{1} \left[\log_2\left(n_{i,\mathrm{CD33\text{-}}}\right) - \log_2\left(pn_{i,\mathrm{CD133\text{-}}}^{\mathrm{init}}\right) - r_{\mathrm{CD133\text{-}}} t_i\right]^2.$$

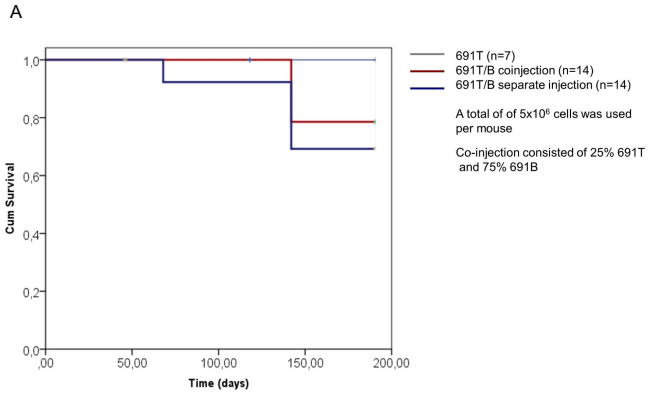

Fig. S2. Kaplan Meier plot showing that co-injection or separate injection of 691 mesenchymal and adrenal cells gives a similar survival of the mice.

With only a single mouse injected with CD133-tumor cells, proper assessment of the uncertainty in the estimated rate parameter is impossible. To obtain a more realistic impression of its uncertainty the noise introduced by boostrapping in the estimation of $r_{\text{CD133+}}$ is transferred to the estimate of $r_{\text{CD133-}}$. In the above, the contribution of the clones to the total number of cells in the tumor is assumed negligible (with seems reasonable in light of the observed data). To reconstruct the time of arrival of each clone, the same exponential growth model as above is employed. In addition, it is assumed that each clone has only a single progenitor cell. The estimated time of arrival of clone k in mouse i is then:

$$\hat{t}_{i,k} = \log_2\left(n_{i,k,\text{CD133+}}\right)/r_{\text{CD133+}}.$$

A 95% confidence interval around each i,k is constructed by sampling from the bootstrap distribution of $r_{\text{CD133+}}$. Similarly, for the clone in the mouse injected with CD133-cells. The estimated probability of proliferation (with 95% C.I.): $p = 4.4 \times 10^{-6}$, (2.05×10^{-6}, 2.015×10^{-5}); the estimated rate of CD133+ proliferation (with 95% C.I.): $r_{\text{CD133+}} = 0.54959$ (0.47359, 0.71215); the estimated rate of CD133-proliferation (with 95% C.I.): $r_{\text{CD133-}} = 0.64582$ (0.56485, 0.80946); the estimated clonal arrival times (with their C.I.) are displayed in Figure S2.

References

[1] Stigliani S, Coco S, Moretti S, Oberthuer A, Fischer M, Theissen J, *et al*. High genomic instability predicts survival in metastatic high-risk neuroblastoma. *Neoplasia*, 2012; 14(9): 823-832.

[2] Aquino VM, Rogers ZR. 50 Years Ago in The Journal of Pediatrics: Neuroblastoma. *J Pediatr*, 2012; 161(3): 416.

[3] Ishimoto H, Jaffe RB. Development and function of the human fetal adrenal cortex: a key component in the feto-placental unit. *Endocr Rev*, 2011; 32(3): 317-355.

[4] Miller RW, L Young Jr. J, Novakovic B. Childhood cancer. *Cancer*, 1995; 75(S1): 395-405.

[5] Schulte M, Köster J, Rahmann S, Schramm A. Cancer evolution, mutations, and clonal selection in relapse neuroblastoma. *Cell Tissue Res*, 2018; 372(2): 263-268.

[6] van Groningen T, Koster J, Valentijn LJ, Zwijnenburg DA, Akogul N, Hasselt NE, *et al*. Neuroblastoma is composed of two super-enhancer-associated differentiation states. *Nat Genet*, 2017; 49: 1261.

[7] Betters E, Liu Y, Kjaeldgaard A, Sundström E, García-Castro MI. Analysis of early human neural crest development. *Dev Biol*, 2010; 344(2): 578-592.

[8] Huber K. Segregation of neuronal and neuroendocrine differentiation in the sympathoadrenal lineage. *Cell Tissue Res*, 2015; 359(1): 333-341.

[9] Calbo J, van Montfort E, Proost N, van Drunen E, Beverloo HB, Meuwissen R, *et al*. A Functional Role for Tumor Cell Heterogeneity in a Mouse Model of Small Cell Lung Cancer. *Cancer Cell*, 2011; 19(2): 244-256.

[10] Brabletz T. To differentiate or not — routes towards metastasis. *Nat Rev Cancer*, 2012; 12: 425.

[11] Aguirre-Ghiso JA. Models, mechanisms and clinical evidence for cancer dormancy. *Nat Rev Cancer*, 2007; 7: 834.

[12] Ocaña OH, Córcoles R, Fabra Á., Moreno-Bueno G, Acloque H, Vega S, *et al*. Metastatic Colonization Requires the Repression of the Epithelial-Mesenchymal Transition Inducer Prrx1. *Cancer Cell*, 2012; 22(6): 709-724.

[13] Thiery JP, Lim CT. Tumor Dissemination: An EMT Affair. *Cancer Cell*, 2013; 23(3): 272-273.

[14] Kemper K, de Goeje PL, Peeper DS, van Amerongen R. Phenotype Switching: Tumor Cell Plasticity as a Resistance Mechanism and Target for Therapy. *Cancer Res*, 2014; 74(21): 5937-5941.

[15] Singh A, Settleman J. EMT, cancer stem cells and drug resistance: an emerging axis of evil in the war on cancer. *Oncogene*, 2010; 29: 4741.

[16] C. Ciccarone V, Spengler BA, Meyers MB, Biedler JL, Ross RA. *Phenotypic Diversification in Human Neuroblastoma Cells: Expression of Distinct Neural Crest Lineages1*. vol. 49. 1989.

[17] Biedler JL, Spengler BA, Chang TD, Ross RA. Transdifferentiation of human neuroblastoma cells results in coordinate loss of neuronal and malignant properties. *Prog Clin Biol Res*, 1988; 271: 265-276.

[18] Ross RA, Spengler BA, Domenech C, Porubcin M, Rettig WJ, Biedler JL. *Human neuroblastoma I-type cells are malignant neural crest stem cells*. vol. 6. 1995.

[19] Walton JD, Kattan DR, Thomas SK, Spengler BA, Guo H-F, Biedler JL, *et al*. Characteristics of stem cells from human neuroblastoma cell lines and in tumors. *Neoplasia*, 2004; 6(6): 838-845.

[20] Han KH, Ro H, Hong JH, Lee EM, Cho B, Yeom HJ, *et al*. Immunosuppressive mechanisms of embryonic stem cells and mesenchymal stem cells in alloimmune response. *Transpl Immunol*, 2011; 25(1): 7-15.

[21] Spengler BA, Lazarova D, Ross RA, Biedler JL. *Cell lineage and differentiation state are primary determinants of MYCN gene expression and malignant potential in human neuroblastoma cells*. vol. 9. 1997.

[22] Bate-Eya LT, Ebus ME, Koster J, den Hartog IJM, Zwijnenburg DA, Schild L, *et al*. Newly-derived neuroblastoma cell lines propagated in serum-free media recapitulate the genotype and phenotype of primary neuroblastoma tumours. *Eur J Cancer*, 2014; 50(3): 628-637.